

Inclusive and exclusive $b \rightarrow s/d\gamma$

N. Taniguchi
 Kyoto University, Kyoto, Japan

In this article, I review the recent results for inclusive and exclusive measurements for $b \rightarrow s\gamma$ and $b \rightarrow d\gamma$ decays from B factories Belle and Babar. I describe the measurement of branching fraction and direct CP violating asymmetry for inclusive $B \rightarrow X_s\gamma$ decay. For results of $b \rightarrow d\gamma$ process, I introduce the measurement of branching fraction of exclusive $b \rightarrow d\gamma$ modes, the first measurement for CP asymmetry of $b \rightarrow d\gamma$ process using $B \rightarrow \rho\gamma$ mode, and semi-inclusive measurement for $B \rightarrow X_d\gamma$.

1. Introduction

Flavor changing neutral currents (FCNC) are forbidden at the tree level in the Standard Model. However, loop-induced FCNC (called penguin decays) are possible. For B meson, two penguin transitions are possible, $b \rightarrow d$ and $b \rightarrow s$, proceeding with a loop where a W and an up-type quark are involved. Figure 1 shows the loop diagram for the $b \rightarrow t \rightarrow (s, d)$ transition. These loop diagrams are quite sensitive to new physics [1]. In order to conserve energy and

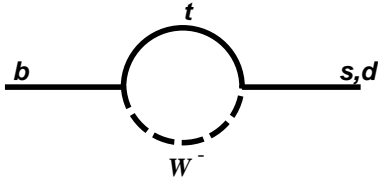


Figure 1: $b \rightarrow (s, d)$ loop(penguin) diagram.

momentum, an additional particle has to be emitted in the transition. In radiative penguin decays (such as $b \rightarrow s\gamma$), a charged particle emits an external real photon.

The $b \rightarrow d\gamma$ process is further suppressed by $|V_{td}/V_{ts}|^2$ and give an alternative to $B^0 - \bar{B}^0$ mixings for extracting $|V_{td}|$. Experimentally, inclusive measurement has large background from the dominant $b \rightarrow s\gamma$ decays which must be rejected using excellent particle identification or kinematic separation. As this process is suppressed in the Standard Model, they provide a good opportunity to look for non-Standard Model effects.

2. Common analysis techniques

The high energy photon is an excellent experimental signature of the fully inclusive measurement. The main background source comes from continuum events ($e^+e^- \rightarrow q\bar{q}(\gamma)$, $q = u, d, s, c$). To suppress the continuum background, we use a selection criteria making use of the difference of the event topology between

B decays and continuum events. These continuum backgrounds are subtracted using the off-resonance data sample taken slightly below the $\Upsilon(4S)$ resonance. In the exclusive measurements, one can require the kinematic constraints on the beam-energy constrained mass $M_{bc} = \sqrt{E_{\text{beam}}^* - p_B^*}$ (also denoted as the beam-energy substituted mass m_{ES}) and $\Delta E = E_B^* - E_{\text{beam}}^*$, using the beam energy E_{beam}^* and momentum p_B^* and E_B^* of B candidate in the center-of-mass frame (c.m.).

3. $b \rightarrow s\gamma$

3.1. Branching fraction of inclusive

$B \rightarrow X_s\gamma$

The Standard Model calculation up to NNLO predicts $\mathcal{B}(B \rightarrow X_s\gamma) = (3.15 \pm 0.23) \times 10^{-4}$ [2] and $\mathcal{B}(B \rightarrow X_d\gamma) = (2.98 \pm 0.26) \times 10^{-4}$ [3]. Agreement between theory and experiment, the world average $(3.55 \pm 0.26) \times 10^{-4}$, has been degraded. Belle group reported a fully inclusive measurement of the $B \rightarrow X_s\gamma$ using $657 \times 10^6 B\bar{B}$ pairs [4]. Another data sample of 68.3 fb^{-1} has been taken at an energy below the resonance and is used to estimate the continuum background. The latter data sample is referred to as OFF sample, while the data taken at $\Upsilon(4S)$ is referred to as ON data.

The strategy for extraction of the E_γ spectrum in the $B \rightarrow X_s\gamma$ is to select all high energy photons, vetoing those originated from decays of $\pi^0 \rightarrow \gamma\gamma$ and $\eta \rightarrow \gamma\gamma$. The continuum background and QED type events are subtracted using the OFF sample. The remaining background from $B\bar{B}$ events are subtracted using Monte Carlo (MC) distributions corrected by control sample data.

Photon candidates are selected from clusters in Electromagnetic calorimeter. They are required to have c.m. energy $E_\gamma^* > 1.4 \text{ GeV}$ and their shower shape to be consistent with and electromagnetic shower. To veto contributions from π^0 and η , each photon candidate is combined with all other photons and invariant mass is calculated. The veto is applied on the likelihood ratio calculated based on the invariant mass and energy of another photon.

Contribution	Fraction
Signal	0.190
Decays of π^0	0.474
Decays of η	0.163
Other secondary γ	0.081
Mis-IDed electrons	0.061
Mis-IDed hadrons	0.017
Beam background	0.013

Table I Relative contributions of the $B\bar{B}$ backgrounds after selection in the $1.7 < E_\gamma^*/(\text{GeV}) < 2.8$ range.

The continuum background are subtracted after scaled by the luminosity, cross section and selection efficiency. In addition, slightly lower mean energy and multiplicity of particles in OFF compared to ON data are corrected. Figure 2 shows the ON and OFF spectra and their difference.

Then, six background categories from B decays are subtracted: (i) photons from $\pi^0 \rightarrow \gamma\gamma$; (ii) photons from $\eta \rightarrow \gamma\gamma$; (iii) other real photons, mainly decays of ω , η' , and J/ψ , and bremsstrahlung, including the short distance radiative correction (modeled with PHOTOS [5]); (iv) cluster in calorimeter not due to single photons (mainly K_L^0 's and neutron's); (v) electrons mis-identified as photons; (vi) beam background. The spectra of the background of photons from B decays with respect to the expected signal events is shown in Figure 3 and listed in Table I.

For each six background categories, photon energy dependent selection efficiency is determined using control sample and the predicted backgrounds from MC are scaled according to the efficiency ratio of data and MC samples.

After subtractions of all backgrounds, photon energy spectrum of signal is obtained. The extracted spectrum is shown in Figure 4. In the range of $1.7 < E_\gamma^* < 2.8$ GeV in the rest frame of the B meson, the results of a partial branching fraction, and the first two moments of the energy spectrum are

$$\mathcal{B}(B \rightarrow X_s \gamma) = (3.31 \pm 0.19 \pm 0.37 \pm 0.01) \times 10^{-4}$$

$$\langle E_\gamma \rangle = 2.281 \pm 0.032 \pm 0.053 \pm 0.002 \text{ GeV}$$

$$\langle E_\gamma^2 \rangle - \langle E_\gamma \rangle^2 = 0.0396 \pm 0.0156 \pm 0.0214 \pm 0.0012 \text{ GeV}^2.$$

In this analysis, the photon energy cut is extended down to 1.7 GeV, which is corresponding to 97% of the spectrum. This result is the most precise measurements to date.

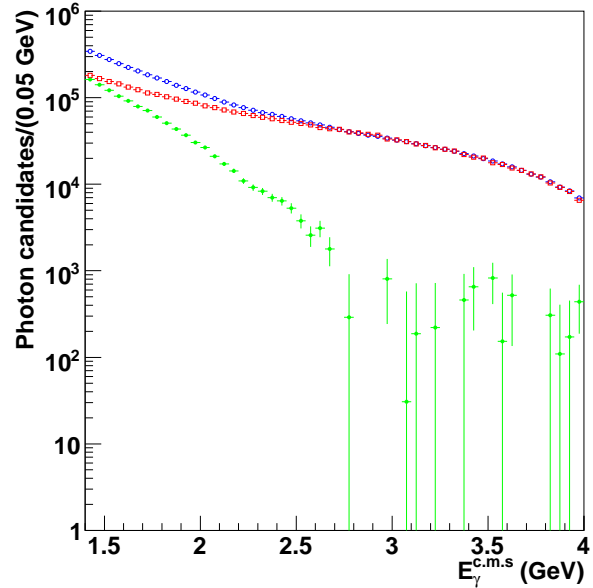


Figure 2: ON data (open circle), scaled OFF data (open square) and continuum background subtracted (filled circle) photon energy spectra of candidates in the c.m.s. frame.

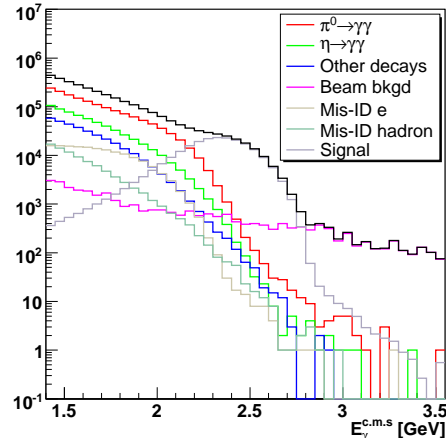


Figure 3: The spectra of photons from B -meson decays passing selection criteria as predicted using a MC sample.

3.2. Direct CP violating asymmetry for inclusive $B \rightarrow X_s \gamma$

Direct CP violating asymmetry is measured using a sample of 383×10^6 $B\bar{B}$ pairs collected with the PEP-II B factory and Babar detector [6]. 16 exclusive $b \rightarrow s\gamma$ final states are reconstructed and the yield asymmetry with respect to their charge conjugate decays $\bar{b} \rightarrow \bar{s}\gamma$ is measured. The hadronic system

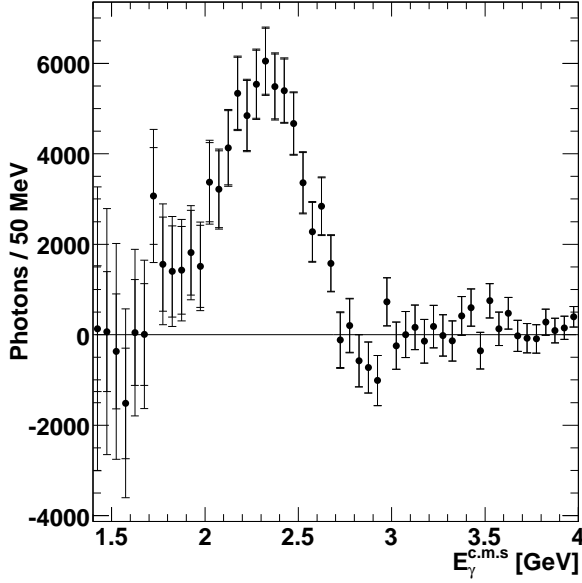


Figure 4: The extracted photon energy spectrum of $B \rightarrow X_{s,d}\gamma$. The two error bars show the statistical and total errors.

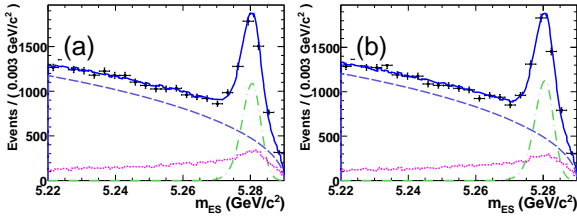


Figure 5: Fits to the m_{ES} distribution in data for (a) $b \rightarrow s\gamma$ events in and (b) $\bar{b} \rightarrow \bar{s}\gamma$ events in the entire M_{X_s} region. The dashed line shows the shape of the continuum, dotted-dashed line shows the fitted signal shape, the dotted line shows the $B\bar{B}$ and cross-feed shape and the solid line shows total.

X_s , formed the kaons and pions, is required to have invariant mass M_{X_s} between 0.6 and 2.8 GeV/c^2 corresponding to a photon energy threshold $E_\gamma > 1.90$ GeV in the B meson rest frame. In this region, the direct CP violating asymmetry in $b \rightarrow s\gamma$ to be $A_{CP} = -0.011 \pm 0.030 \pm 0.014$. This result is the most accurate measurement of this quantity to date. It is consistent with zero CP violating asymmetry and the SM prediction. Figure 5 shows the m_{ES} distribution in data for $b \rightarrow s\gamma$ and $\bar{b} \rightarrow \bar{s}\gamma$ events.

4. $b \rightarrow d\gamma$

4.1. Branching fraction of exclusive $b \rightarrow d\gamma$ modes

The exclusive measurements of $b \rightarrow d\gamma$ are improved by Belle. The branching fractions for $B \rightarrow \rho\gamma$ and $B \rightarrow \omega\gamma$ are measured using 657×10^6 $B\bar{B}$ pairs [8]. The results are $\mathcal{B}(B^+ \rightarrow \rho^+\gamma) = (8.7^{+2.9+0.9}_{-2.7-1.1}) \times 10^{-7}$, $\mathcal{B}(B^0 \rightarrow \rho^0\gamma) = (7.8^{+1.7+0.9}_{-1.6-1.0}) \times 10^{-7}$, and $\mathcal{B}(B^0 \rightarrow \omega\gamma) = (4.0^{+1.9}_{-1.7} \pm 1.3) \times 10^{-7}$. The results of the fits are shown in Fig. 6. Three $\rho\gamma$ and $\omega\gamma$ modes are combined assuming a single branching fraction $\mathcal{B}(B \rightarrow (\rho, \omega)\gamma) \equiv \mathcal{B}(B^+ \rightarrow \rho^+\gamma) = 2 \frac{\tau_{B^+}}{\tau_{B^0}} \mathcal{B}(B^0 \rightarrow \rho^0\gamma) = 2 \frac{\tau_{B^+}}{\tau_{B^0}} \mathcal{B}(B^0 \rightarrow \omega\gamma)$, where $\frac{\tau_{B^+}}{\tau_{B^0}} = 1.071 \pm 0.009$. The combined results are $\mathcal{B}(B \rightarrow \rho\gamma) = 12.1^{+2.4}_{-2.2} \pm 1.2$ and $\mathcal{B}(B \rightarrow (\rho, \omega)\gamma) = 11.4 \pm 2.0^{+1.0}_{-1.2}$.

The ratios of the branching fractions of the $B \rightarrow \rho\gamma/\omega\gamma$ modes to those of the $B \rightarrow K^*\gamma$ modes can be related to $|V_{td}/V_{ts}|$. The calculated ratio to be

$$\frac{\mathcal{B}(B \rightarrow (\rho, \omega)\gamma)}{\mathcal{B}(B \rightarrow K^*\gamma)} = 0.0284 \pm 0.0050^{+0.0027}_{-0.0029}. \quad (1)$$

Using the prescription in Ref. [7], Eq. 1, for example, gives $|V_{td}/V_{ts}| = 0.195^{+0.020}_{-0.019}(exp) \pm 0.015(th)$. This is consistent with determinations from $B^0 - \bar{B}^0$ and $B_s^0 - \bar{B}_s^0$ mixings [7], which involve box diagrams rather than penguin loop.

4.2. CP asymmetry for $B \rightarrow \rho\gamma$

The first measurements of CP -violating asymmetries in $b \rightarrow d\gamma$ are reported by Belle. The CP -violating parameters in $B^0 \rightarrow \rho^0\gamma$ decays [9] and charge asymmetry in $B^+ \rightarrow \rho^+\gamma$ [8] are measured. In the decay $B^0 \rightarrow \rho^0\gamma$, the Standard Model predicts no time-dependent CP asymmetry (\mathcal{S}) and -0.1 for the direct CP asymmetry (\mathcal{A}) [10, 11, 12, 13]. Assuming the top quark is the dominant contribution in the loop diagram, the decay amplitude has a weak phase that cancels the phase in the mixing; consequently \mathcal{S} vanishes. Observing a non-zero of \mathcal{S} would indicate effects of new physics with new CP violating phase and right-handed current. The direct CP -violating asymmetry in $B^+ \rightarrow \rho^+\gamma$ is induced due to an additional contribution from an annihilation diagrams and predicted to be -0.1 in the Standard Model predictions [14].

Figure 7 shows the Δt distributions and the raw asymmetry for good tag quality events. Δt is difference of decay time of B meson pairs and the b -flavor charge $q = +1(-1)$ when the tagging B meson is a $B^0(\bar{B}^0)$.

The results of CP -violating parameters are $\mathcal{S}_{\rho^0\gamma} = -0.83 \pm 0.65 \pm 0.18$ and $\mathcal{A}_{\rho^0\gamma} = -0.44 \pm 0.49 \pm 0.14$,

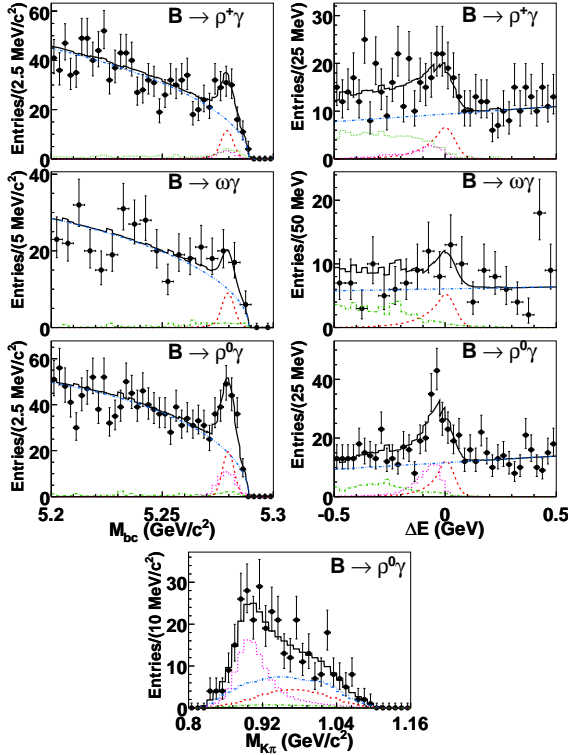


Figure 6: Projections of the fit results to M_{bc} (in $|\Delta E| < 0.1$ GeV and $0.92 \text{ GeV}/c^2 < M_{K\pi}$), ΔE (in $5.273 \text{ GeV}/c^2 < M_{bc} < 5.285 \text{ GeV}/c^2$ and $0.92 \text{ GeV}/c^2 < M_{K\pi}$), and for $B^0 \rightarrow \rho^0\gamma$, $M_{K\pi}$. Curves show the signal (dashed, red), continuum (dot-dot-dashed, blue), $B \rightarrow K^*\gamma$ (dotted, magenta), other backgrounds (dash-dotted, green), and the total fit result (solid).

and the charge asymmetry is $A_{CP}(B^+ \rightarrow \rho^+\gamma) = -0.11 \pm 0.32 \pm 0.09$. Both results are consistent with SM predictions, but also consistent with no CP asymmetry due to the large errors. These are the first measurements of CP -violating asymmetries in a $b \rightarrow d\gamma$ process.

4.3. Sum of exclusive modes

Recently Babar reported preliminary results of a search for $B \rightarrow X_d\gamma$ decays with a hadronic mass $1.0 < M_{X_d} < 1.8 \text{ GeV}/c^2$ [15]. Seven final states with up to four charged pions and one neutral pion or η are considered. It corresponds to about 50% of the total X_d fragmentation in this mass range, in which $B \rightarrow \rho\gamma$ and $\omega\gamma$ are not included. Figure 8 shows signal distributions of m_{ES} and ΔE in the range $1.0 \text{ GeV}/c^2 < M_{X_d} < 1.8 \text{ GeV}/c^2$ with the background subtraction.

The partial branching fraction is

$$\mathcal{B}(B \rightarrow X_d\gamma) = (3.1 \pm 0.9 \pm 0.7) \times 10^{-6}.$$

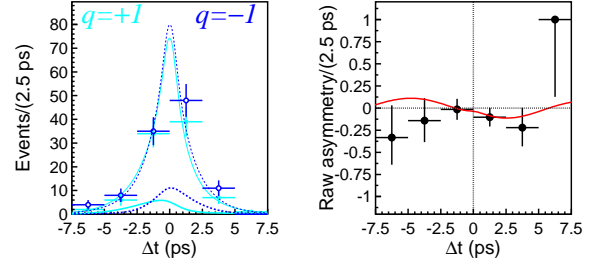


Figure 7: (Left) Δt distributions for $B^0 \rightarrow \rho^0\gamma$ for $q = +1$ (light solid) and $q = -1$ (dark dashed) for good b -flavor tag quality events. The thin curve is the fit projection while the thick curve shows the signal component. Points with error bars are data. (Right) Raw asymmetry in each Δt bin for good b -flavor tag quality events. The solid curve shows the result of the fit.

This is promising method for improved $|V_{td}/V_{ts}|$ determination.

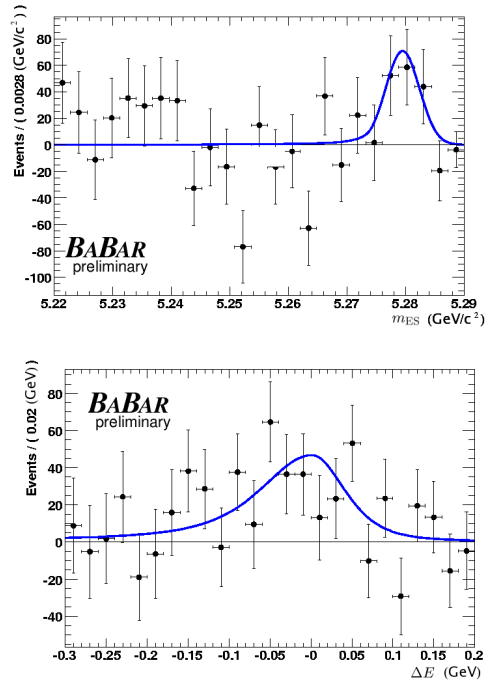


Figure 8: Signal distributions of m_{ES} (up) and ΔE (bottom) for $B \rightarrow X_d\gamma$ in the range $1.0 \text{ GeV}/c^2 < M_{X_d} < 1.8 \text{ GeV}/c^2$ with the background subtraction. The curves represent the PDFs used in the fit, normalized to the fitted yield.

5. Conclusion

For $b \rightarrow s\gamma$ inclusive analysis, the branching fraction and CP -violating asymmetry are precisely mea-

sured. For $b \rightarrow d\gamma$, exclusive modes are measured with large data sample. The CP -violating asymmetries in $b \rightarrow d\gamma$ process are first measured with $B \rightarrow \rho\gamma$ modes. The branching fraction of $B \rightarrow X_d\gamma$ are also first measured in the range $1.0 \text{ GeV}/c^2 < M_{X_d} < 1.8 \text{ GeV}/c^2$.

References

- [1] For example, A. Arhrib, C.-K. Chua and W.-S. Hou, Eur. Phys. J. C **21**, 567 (2001); A. Ali and E. Lunghi, Eur. Phys. J. C **26**, 195 (2002); Z.-J. Xiao and C. Zhuang, Eur. Phys. J. C **33**, 349 (2004).
- [2] M. Misiak *et al.*, Phys. Rev. Lett. **98**, 022002 (2007).
- [3] T. Becher, M. Neubert, Phys. Rev. Lett. **98**, 022003 (2007), For other NNLO calculations, see e.g., J.R. Andersen, E. Gardi, JHEP 0701:029 (2007).
- [4] Belle Collaboration, K. Abe *et al.*, arXiv:0804.1580[hep-ex].
- [5] E. Barberio *et al.*, Heavy Flavor Averaging Group (HFAG), arXiv:0704.3575 [hep-ex] (2007).
- [6] BABAR Collaboration: B. Aubert, *et al.*, arXiv:0805.4796 [hep-ex](2008) .
- [7] CDF - Run II Collaboration, A. Abulencia *et al.*, Phys. Rev. Lett. **97**, 062003 (2006).
- [8] N. Taniguchi, M. Nakao, S. Nishida *et al.*. (The Belle collaboration), Phys. Rev. Lett. **101**, 111801 (2008).
- [9] Y. Ushiroda, K. Sumisawa, N. Taniguchi *et al.*. (The Belle collaboration), Phys. Rev. Lett. **100**, 021602 (2008).
- [10] A. Ali and A. Parkhomenko, Eur. Phys. J. C **23**, 89 (2002); See updated calculations in A. Ali and A. Parkhomenko, (2006), hep-ph/0610149.
- [11] M. Beneke, T. Feldmann and D. Seidel, Eur. Phys. J. C **41**, 173 (2005).
- [12] S. Bosch and G. Buchalla, Nucl. Phys. B **621**, 459 (2002); See updated calculations in S. Bosch and G. Buchalla, JHEP, 051:035, (2005).
- [13] P. Ball, G.W. Jones, and R. Zwicky, Phys. Rev. D **75**, 054004 (2007).
- [14] Z.-J. Xiao and C. Zhuang, Eur. Phys. J. C **33**, 349 (2004).
- [15] BABAR Collaboration: B. Aubert, *et al.*, arXiv:0708.1652 [hep-ex] (2007).